Available online at www.eccomasproceedia.org
Eccomas Proceedia COMPDYN (2023) 5300-5313

ECCOMAS
Proceedia

COMPDYN 2023
9th ECCOMAS Thematic Conference on
Computational Methods in Structural Dynamics and Earthquake Engineering
M. Papadrakakis, M. Fragiadakis (eds.)
Athens, Greece, 12-14 June 2023

EARTHQUAKE NATECH RISK: NUMERICAL ANALYSIS OF FLOATING ROOF AND SEALING SYSTEM IN CYLINDRICAL STORAGE TANKS

Michela Salimbeni[1], Maurizio De Angelis[1], and Mariano Ciucci[2]

[1] La Sapienza University of Rome
e-mail: {michela.salimbeni,maurizio.deangelis}@uniroma1.it

[2] INAIL (Italian National Institute for Insurance against Accidents at Work), DIT
m.ciucci@inail.it

Abstract

Earthquake is one of the natural event that are part of NaTech events (Natural Hazard Triggering Technological Disasters). Cylindrical liquid storage tanks with floating roof are common equipment in industrial plants, and they are vulnerable to earthquakes. In fact, seismic damage to tanks with floating roof can lead to major accidents involving hazardous substances, mainly due to convective fluid movement and to the interactions between the tank wall, the fluid, the floating roof, the sealing system, and the bumper bars. In rim seal fires, which occur when the sealing system is damaged and an impact occurs between the bumper bars and the tank wall, the horizontal dynamics of the floating roof is involved. The horizontal dynamics depends mainly on the mechanical characteristics of the sealing system and the type of impact.
The objective is to predict the horizontal vibration response of the floating roof of a tank subjected to seismic excitation, taking into account different boundary conditions. For this purpose, a simplified and reduced model is developed assuming a decoupling hypothesis between the horizontal and the vertical motion of the roof. Different types of sealing systems (i.e., different mechanical properties) are investigated, considering the possibility of impact between the bumper bars and the tank wall. This impact is usually rigid. Later, as a proposal for the prevention of major accidents, deformable bumpers are introduced to reduce the maximum contact force and avoid the impact between two metallic parts.

Keywords: Earthquake NaTech risk, major-hazard industrial plants, storage tanks, floating roof, sealing system, bumper, Finite Element Model, hard impact, soft impact.

ISSN:2623-3347
Peer-review under responsibility of the organizing committee of COMPDYN 2023.
doi: 10.7712/120123.10801.21314

1 INTRODUCTION

Seismic events in the past have shown that industrial plants are vulnerable to the earthquake. Their vulnerability results from the complexity of the layout: they are characterized by many connections, equipment and components which, combined with the complexity of their operations, make them highly susceptible to seismic excitation. This implies the possibility of accidental chains forming, with a possible domino effect, which can cause explosions, fires and releases of dangerous substances treated by the industrial processes. In cases where natural disasters interact with industrial risk, this is referred to as NaTech events (Natural Hazard Triggering Technological Disasters). Among the NaTech events, the earthquake is one of the most significant, it simultaneously affects the entire plant, and it can cause simultaneous damages to equipment [1,3]. In terms of safety, in Italy industrial plants that operate with hazardous substances are called "major hazard industrial plants" and are subject to Italian standard D.Lgs. 105/2015, transposition of Directive 2012/18/EC – Seveso III.

One of the typical equipment in major hazard industrial plants is the cylindrical liquid storage tanks with floating roof [4]. Seismic damages to the floating roof and non-structural elements can cause hazardous substance releases, fires and explosions.

The floating roof is a circular steel structure equipped with floating caissons that allow it to float above the product stored. A space between the outer edge of the roof and the inside of the tank shell, 200 mm in size, is closed by means of a flexible sealing system. Also, there are limiting bumper bars to guarantee the protection of the sealing system in case of large displacement.

As a part of major accidents, rim seal fire is the most common type of fire in a tank with floating roof. This occurs when the sealing system is damaged, loses its integrity and allows the leakage of vapors that can be ignited [5]. These vapors can be ignited by sparks from impact between bumper bars and the tank wall, two metallic parts. In this framework, the horizontal dynamics of the roof with the sealing system and with the bumper bars is of particular interest for the earthquake NaTech risk assessment of atmospheric tanks with floating roofs.

In Literature, before the 1950s, the floating roof was regarded as a non-structural element and its contribution to the response was limited to an increase in damping; all design was based on theories proposed by Jacobsen [6], Senda [7] and Nakagawa [8] for cylindrical tanks. In Nakagawa [8] the roof was modelled as a rigid plate whit mass, and linear potential theory was applied to solve the fluid-roof interaction problem. Subsequently, in Sakai et al [9] the roof was modelled with an elastic plate with mass, still remaining within the framework of the elastic potential theory. Other authors then dealt with the non-linear aspects of the problem [10,11]. In [12], Matsui presented an analytical solution to predict the sloshing response of a cylindrical liquid storage tank with floating roof under seismic excitation. The author assumed the liquid as inviscid, incompressible, and irrotational, while the floating roof was modeled as an isotropic elastic plate with uniform stiffness and mass. The dynamic interaction between the liquid and the floating roof was considered exactly within the framework of linear potential theory. In [13], Matsui derived an analytical solution for sloshing in a cylindrical liquid storage tank with a single-pontoon floating roof under seismic excitation. Under the same hypothesis and in the same linear framework, the author considered the floating roof composed of an inner deck, which may be idealized as an isotropic elastic plate with uniform thickness and mass, and connected to an outer pontoon, which is modeled as anelastic curved beam. In [12,13], Matsui imposed the free-boundary conditions along the roof edge. Shabani and Golzar [14] investigated the sloshing response of the floating roofs for different ground motion records taking into account the nonlinearity due to large deflection of the deck plate. Free-boundary conditions were required on the roof edge. Hosseini et al [15] proposed a simplified numerical method for

modeling the interaction between the floating roof and the tank wall. The authors assumed that sloshing was suppressed by the presence of the roof, and they modeled the sealing system through pre-compressed only-compression radial springs all around the roof. For the case study, the deformation of the tank wall is comparable with the nominal gap covered by the sealing system. A finite element model was presented in [16], that validated the analytical model presented in [15]. Caprinozzi et al. in [16] were interested to predict the maximum vertical displacement of the roof in order to carry on a seismic fragility analysis for the liquid overtopping. The interaction between the edge of floating roof and the tank wall was frictionless in tangential direction and 'hard contact' type in radial direction. Ahmadi et al [17] modeled a cylindrical tank with floating roof with two different type of sealing system. The authors investigated the effect of friction and damping of the sealing system on the vertical seismic response of the floating roof.

Thus, the vertical response of the floating roof over time has been extensively studied, in some cases taking into account also the presence of the sealing system. On the contrary, the horizontal response of the floating roof has not been discussed yet.

Prediction of the horizontal dynamic response of the floating roof of a tank subject to seismic excitation at the base allows the assessment, the monitoring and the mitigation of the seismic risk. Indeed, some proposals for monitoring have already been made in [18], so models that describe the horizontal dynamics of the roof would be used to estimate some risk thresholds for the activation of early warning systems. In addition, some efforts have already been made in the field of passive seismic protection of industrial components [19], and in particular of the floating roof by Zahedin Labaf et al. in [20], in which a hybrid control system is proposed, where a base isolation system is equipped with a tuned mass damper inerter. This system was experimentally tested in [21].

In this study, the horizontal dynamics of the floating roof with sealing system and bumper bars is the subject of interest. In particular, in the field of impact dynamics, in [22] and [23] the use of collision buffers is proposed for the attenuation of structural pounding in case of earthquakes.

The first purpose is the realization of a simplified and reduced model in order to carry out effortless analyses, without having to rely on a comprehensive model of the type that already exists in the Literature. By the assumption of decoupling between the vertical and horizontal motion of the roof, the geometric and mechanical properties of the tank that characterize the horizontal dynamics are highlighted.

The second purpose concerns the influence of some parameters on the horizontal dynamic response of the roof. As a preliminary study, a parametric analysis is presented, considering the impact between the bumpers and the tank wall. In a first step, the impact is considered as rigid elastic. Then, the hypothesis of partially deformable bumper bars is introduced, which leads to soft elastic impact.

The paper is organized as follows. Section 2 describes the main characteristics of the elements that constitute the tanks with floating roof. Section 3 explains the assumptions underlying the parametric analyses and the simplified model. Section 4 presents a detailed description of the finite element model. Sections 5 and 6 contain the parametric analyses and the results obtained considering, respectively, the elastic hard impact and the elastic soft impact.

2 CYLINDRICAL LIQUID STORAGE TANKS WITH FLOATING ROOF

2.1. Floating roof

Tanks with floating roof are used for the storage of volatile products. The roof is located on the surface of the product and, by sliding vertically along the shell for product inlet / outlet, ensures that most of the vapor remains contained under the roof.

The roof is a circular steel structure with floating caissons that allow it to float above the product stored. Generally, the diameter of the floating roof is about 400 mm smaller than the inside diameter of the tank. The space between the outer edge of the roof and the inside of the tank shell is closed by a flexible sealing system, which also allows the position of the roof in the tank to be centralized. There are two main types of floating roof, single pontoon and double pontoon. The single pontoon roof owns its inherent buoyancy to an outer annular pontoon, while the central part is formed by a membrane of steel plates welded together and connected to the inner edge of the caissons. The double pontoon roof consists of an upper and lower steel membrane separated by a series of radially divided circumferential stiffeners.

Also, some elements are required for the functionality of the tank, such as flexible piping systems, edge vents, rain drainage system, roof supports, guide pipe, stilling pipe and floating roof sealing system.

2.2. Sealing systems

The rim seal must be sufficiently flexible for different reasons:

- to adapt to possible construction irregularities, given by the large size of the elements between which it is inserted;
- to limit the possibility of impact between steel parts;
- to recenter the roof during the operation phases.

In addition, it shall allow the roof to move vertically during the normal operation of the tank.

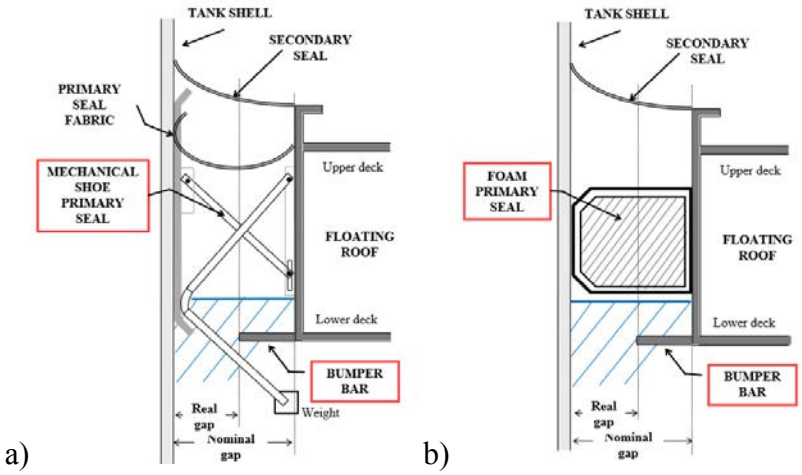

Figure 1: a) Mechanical sealing system, b) Fabric with foam sealing system.

The floating roofs are equipped with the primary and secondary seal: the secondary one is mounted above the primary seal with the aim of minimizing vapor and odor losses. In practical use, different types of sealing rim are currently employed. For primary seal, several solutions are available, including metal shoes (Fig. 1a), non-metallic tubular or fabric seals (Fig. 1b). The working range of sealing systems, as stated by the manufacturers, is usually 205±100 mm. The sealing systems are also installed with initial compression. The initial compression ensures

adherence to the tank wall to prevent the seal from being stretched. Horizontal displacements of the floating roof greater than 205+100 mm will result in excessive compression on one side of the seal and possible separation from the other side of the seal.

2.3. Limiting bumper bars

The seal allows variations of 100 mm in the rim space: excessive deformation of the seal is prevented by limiting bumper bars mounted on the lower edge of the outer rim of the roof. The bars are made of steel.

3 BASIC ASSUMPTIONS

The constituent elements of a tank with floating roof are as follows: the walls and bottom of the tank, the fluid, the floating roof, the sealing system, the bumper bars. A comprehensive model for assessing the seismic response of tank with floating roof should include all the elements listed above. In order to study the only horizontal dynamics of the floating roof, the vertical motion of the roof can be decoupled from the horizontal one. This hypothesis is based on the following assumptions:

- the hypothesis of small vertical displacements of the roof is true;
- there is no tangential action of the fluid transmitted to the floating roof.

By introducing the decoupling hypothesis, it's possible to move from the comprehensive model to a simplified model where only the horizontal dynamics is relevant.

Furthermore, since the stiffness in the roof plane is much greater than the radial stiffness of the sealing system, the roof can be considered as a rigid body. The simplified model is also reduced in the number of the degrees of freedom.

The proposed model is simplified and reduced. In particular, it considers only 1 degree of freedom of the floating roof- the horizontal displacement in the direction of application of the seismic action- and the degrees of freedom of the bumpers, related to their deformation at the impact.

The dynamic parameters that characterize the horizontal response of the roof are as follows:

- m, the mass of the roof,
- k_S and c_S , stiffness and damping coefficient of the sealing system (or damping factor ξ_S),
- k_B and c_B , stiffness and damping coefficient of the bumper bars,
- G_0 the initial gap.

Different scenarios are evaluated by varying k_S, keeping m constant. The damping associated with the sealing system generally depends on the type of sealing system adopted. In this study, the damping of the sealing system is fixed.

The bumper bars are initially considered rigid. The bumpers, which certainly limit the horizontal displacements of the roof and prevent damage to the stop system, can also cause some issues. The punctual and repeated impact of the bars against the tank wall can generate high contact forces. In addition to producing sparks due to the contact between two metallic materials, the impact can also cause damage to the tank. Evaluation of the contact force is therefore useful for local checks of the tank section.

In the second part of the study, the possibility of using partially deformable bumper bars is investigated. By using deformable bumper bars, it is possible to limit the contact forces generated by the impact, both in forced vibrations and in free vibrations. A parametric analysis is performed by varying the stiffness of the bumper k_B, for each scenario of the first part.

The damping of the bumper c_B , also a fundamental parameter in the dynamics of the impact, is assumed to be zero in order to study the contribution of the stiffness of the bumper only. Thus, the impact is considered elastic.

In all analyses, the value of the initial real gap is fixed.

4 FINITE ELEMENT MODEL

Using the finite element software Abaqus/Explicit, a simplified and reduced model of the tank with floating roof shown in the Fig. 2 is developed. The material properties and dimensions of the tank are reported in Tab. 1. The case study is taken from the tank in [19].

The tank is treated as a rigid body (Discrete Rigid Surface); therefore, it has not been assigned any type of material. The roof is a double pontoon type, like that of Matsui in [12], and it is modeled as an equivalent shell, with distributed mass and stiffness. The sealing system is modelled as an annular shell part: the seal is tied to the outer rim of the roof and the to the inner wall tank. The sealing system is discretized using membrane elements with significantly lower in-plane stiffness than the radial stiffness of the roof. The roof can therefore be considered as a rigid body. Different stiffness values k_S are assigned to the sealing system, in terms of the Young's modulus of the material E_S, in order to achieve periods of vibration in a range 3.0-0.5 s. The damping of the sealing system is fixed at 1% in terms of damping factor ξ_S.

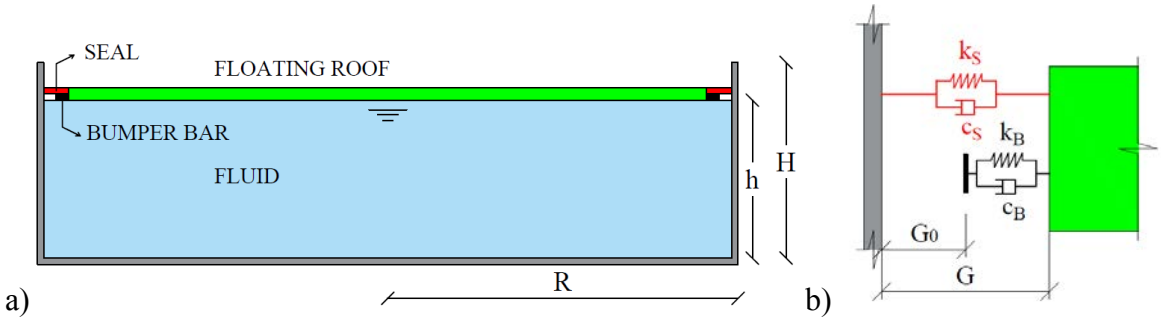

Figure 2: Tank with floating roof: a) a complete model, b) a detail of the simplified and reduced model

Tank's radius R [m]	27.43
Tank's height H [m]	15.60
Fluid's height h [m]	13.60
Density of the roof γ [kg/m^3]	380.00
Thickness of the roof t [m]	0.25
Young's modulus of the roof material E_r [Pa]	2.10×10^{11}
Poisson's coefficient of the roof material ν [-]	0.3
Young's modulus of the seal material E_S [Pa]	various
Damping factor of the seal ξ_S [-]	0.01
Nominal gap G [m]	0.20
Real gap G_0 [m]	various
Linear stiffness of the bumper k_B [N/m]	various
Damping coefficient of the bumper c_B [Ns/m]	0.00

Table 1: Geometrical and mechanical properties of the case study.

The limiting bumper bars are continuously modeled by assigning a contact interaction between the outer edge of the roof and the inner wall of the tank. A thickness property is assigned to the contact, reducing the nominal gap. At first, the bumper bars realize a rigid stop by assigning a frictionless tangential behavior and a "hard contact" normal behavior. Later, the contact behavior in the normal direction is assigned as a bilinear pressure-overclosure relationship.

The value of the initial real gap is always fixed.

The fluid is not modeled, due to the decoupling hypothesis.

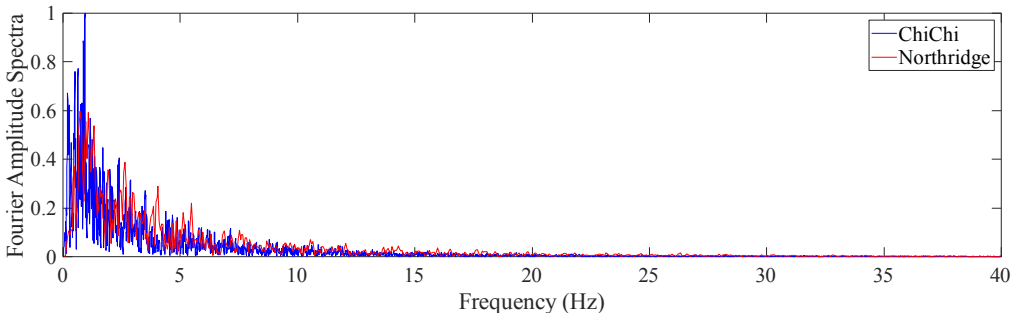

Figure 3: Fourier amplitude spectra of the Northridge and Chi-Chi earthquake.

Two recordings of natural seismic events (Fig. 3) are used to perform the analysis, the Northridge earthquake (1994) and the Chi-Chi earthquake (1999). The seismic excitation is applied in X direction.

5 ELASTIC HARD IMPACT ANALYSIS

5.1. Parametric analysis

A hard impact is a contact that occurs in an infinitely small time between non-deformable collision bodies. Any loss of energy during the impact is represented by a constant value of the coefficient of restitution s, defined as the ratio between the post- (v_f) and pre-impact speeds (v_i):

$$s = v_f / v_i \tag{1}$$

The coefficient of restitution assumes values between 0 (fully plastic contact) and 1 (fully elastic contact).

Without considering any source of energy loss (no damping) and assuming that the collision bodies are rigid, the impact is elastic hard.

The value of the initial gap is set at 100 mm.

Five Young's modulus values have been assigned to the sealing system material, which are reported in Tab. 2.

A representation of the constitutive relation of the reduced model is shown in Fig. 4.

A total of ten analyses are conducted.

E_S [Pa]	1.00E+4	1.85E+4	4.00E+4	1.40E+5	5.00E+5
T_n [s]	3.00	2.25	1.50	0.75	0.50

Table 2: Young's modulus values selected for the seal system for parametric analysis.

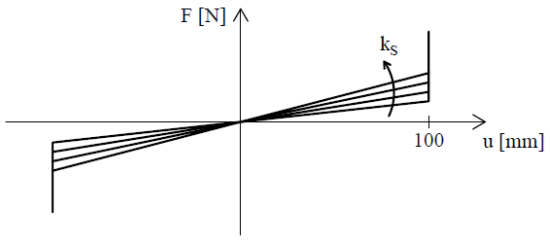

Figure 4: Bilinear force-displacement relationship of the sealing system with rigid bumper bars.

5.2. Results and discussion

The seismic response is reported in terms of horizontal displacements of the floating roof relative to the tank, and of the contact forces that occurs as a result of the impact.

The relative horizontal displacements of the roof $u_r(t)$ can be considered, on the other side, as the deformation of the sealing system $\varepsilon(t)$

$$\varepsilon(t) = \frac{[G - u_r(t)]}{G} \tag{2}$$

where which must not be less than 0.5.

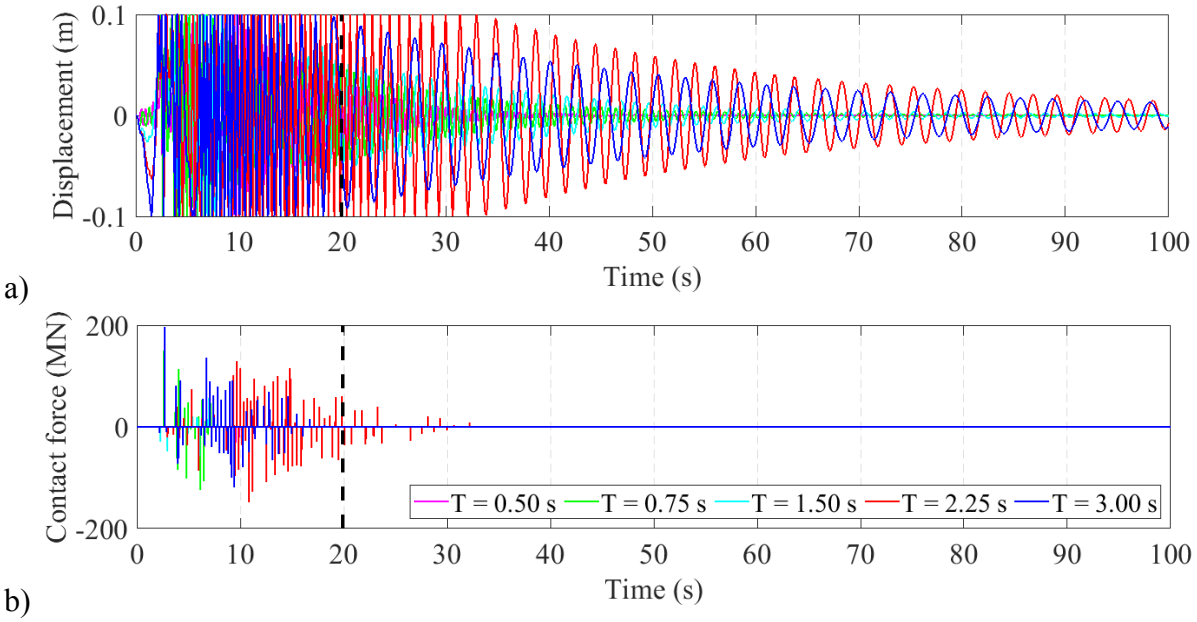

Figure 5: Seismic response for Northridge earthquake for different stiffness of the seal: a) relative displacement of the roof; b) total contact force.

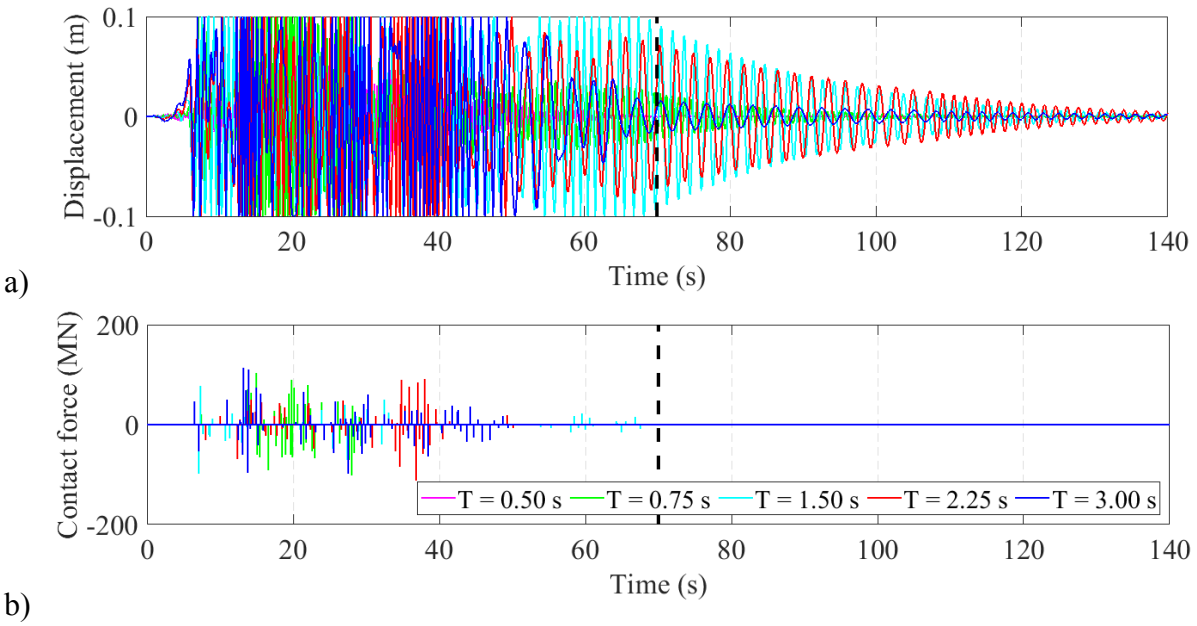

Figure 6: Seismic response for Chi-Chi earthquake for different stiffness of the seal: a) relative displacement of the roof; b) total contact force.

The total contact force it's the integral of the contact pressure on the contact area. The contact force is considered positive when the impact occurs in the +x direction and negative when the impact occurs in the -x direction.

The seismic response is obtained both during forced oscillations and during free oscillations. A black dotted vertical line separates the two phases.

The Northridge earthquake response (Fig. 5) shows that the greatest number of impacts occur during the forced oscillations phase, especially for cases where the sealing system is more deformable. In particular, for T_n = 3.00 seconds, there are also impacts after the end of the earthquake. The number of impacts n_I is variable with the stiffness of the sealing system, while the contact forces remain in the range of 149-197 MN values for all the stiffness values studied, except for the most rigid case, for which only 5 impacts with a contact force value of 53 NM are recorded.

In addition, the free oscillations of the cases where the sealing system is more deformable show a higher roof recentering time, which is more than 80 s for the cases where T_n is equal to 3.00 s, 2.25 s and 1.50 s.

The Chi-Chi earthquake response (Fig. 6) shows that the impact occurs only in the forced oscillation phase. The number of impacts decreases significantly as the stiffness of the sealing system increases, up to the stiffest case with T_n = 0.50 s, where the displacements are always less than the initial gap. Again, for cases where the sealing system is more deformable, there is a longer recentering time of the roof.

From the seismic response to both earthquakes, it is evident that varying the stiffness of the sealing system produces a variation in the number of impacts, the contact force, and the recentering time.

Further studies should be developed to investigate the effect of damping of the sealing system.

EARTHQUAKE	T_n [s]	n_I [-]	$F_{C\max}$ [MN]
Northridge	3.00	46	197.2
	2.25	75	149.0
	1.50	10	151.3
	0.75	18.0	149.8
	0.50	5.0	53.4
Chi-Chi	3.00	73	114.3
	2.25	55	112.5
	1.50	48	97.8
	0.75	38	102.0
	0.50	0	0.0

Table 3: Number of impacts and maximum contact force as a function of the different stiffnesses of the sealing system for the two earthquakes.

6 ELASTIC SOFT IMPACT ANALYSIS

6.1. Parametric analysis

In soft impact the deformation of collision bodies is considered. The phenomenon of contact can be simulated by different laws of force overclosure. The simplest model is represented by the linear spring element, which assumes a linear relationship between the contact force and the overclosure, without taking into account the energy loss during the impact. In this case, the impact is elastic soft.

In the case of partially deformable bumper bars, where the deformable part will be made of non-metallic material, it must be considered that the working range of the sealing systems is 200±100 mm. Therefore, the deformation of the bumpers must be such as to ensure that the displacements of the roof are always within this range.

For this reason, the bumper bars are such that the initial gap G_0 is less than 100 mm, which is equal to 70 mm. The 30 mm difference from the real gap takes into account the partially deformation of the bumper bar. Considering a smaller initial gap will increase the number of impacts while reducing the contact force.

Defining

$$\lambda = \frac{k_B}{k_S} \tag{3}$$

the ratio between the stiffness of the seal and the stiffness of the bumpers, three different values for λ are investigated, for each value of k_S, except for the highest value of k_S, because it's the case where the lower number of impacts are highlighted together with the lower value of maximum contact force. The values for λ are shown in Tab. 4. A total of forty analyses are conducted, keeping $\xi_S = 0.01$.

A representation of the constitutive relation of the reduced model is shown in Fig. 7.

T_n [s]	k_S [N/m]	k_B [N/m]				
		λ=10	λ=100	λ=300	λ=600	λ=1000
3.00	9.71e+5	9.71e+6	9.71e+7	2.91e+8	5.82e+8	9.71e+8
2.25	1.73e+6	1.73e+7	1.73e+8	5.18e+8	1.04e+9	1.73e+9
1.50	3.88e+6	3.88e+7	3.88e+8	1.16e+9	2.33e+9	3.88e+9
0.75	1.55e+7	1.55e+8	1.55e+9	4.66e+9	9.32e+9	1.55e+10

Table 4: λ values selected for parametric analysis.

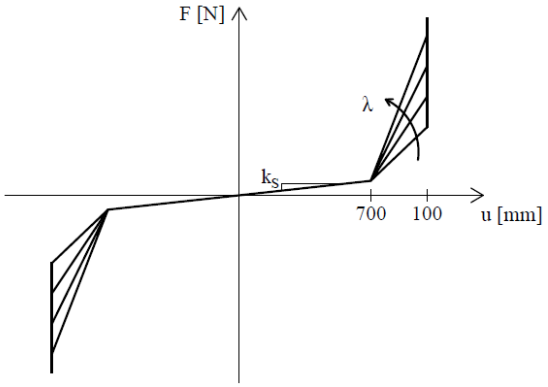

Figure 7: Trilinear force-displacement relationship of the sealing system with deformable bumper bars.

6.2. Results and discussion

Fig. 8 shows the maximum contact force $F_{C,\max}$ for the different values of k_S investigated and for the different λ. These results are compared with the two limit cases of hard impact with G_0 = 100 mm (first group of bars on the left) and G_0 = 70 mm (last group of bars on the right). In fact, the case of $\lambda = 1000$ tends to the hard impact with $G_0 = 70$ mm. On the contrary, at $\lambda = 10$ the stop is sufficiently deformable that, at the limit, it is as if there were no deforming space for the bumper, as if it were a hard impact with $G_0 = 100$ mm.

The trend of the $F_{C,max}$ for the different λ values shows that for λ between 10 and 100, the minimum of $F_{C,max}$ are recorded for almost all k_S. In particular, for more deformable sealing systems, i.e. those associated with higher vibration periods ($T_n = 3.00$ s, $T_n = 2.25$ s), the minimum value of $F_{C,max}$ is recorded for values around $\lambda = 100$. On the other hand, for more rigid systems, the minimum contact force can also be obtained for $\lambda = 10$.

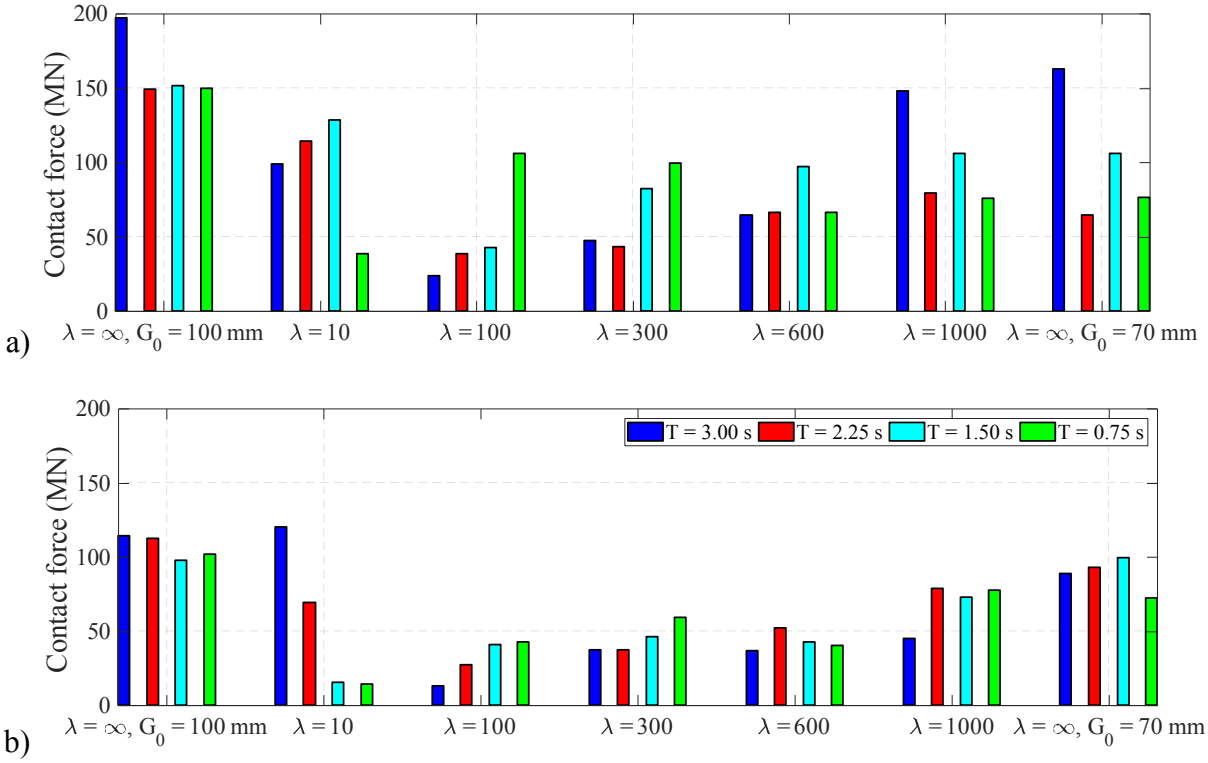

Figure 8: Bar graph of maximum contact force as a function of the different stiffnesses of the sealing system and λ values for the two earthquakes, a) Northridge, b) Chi-Chi.

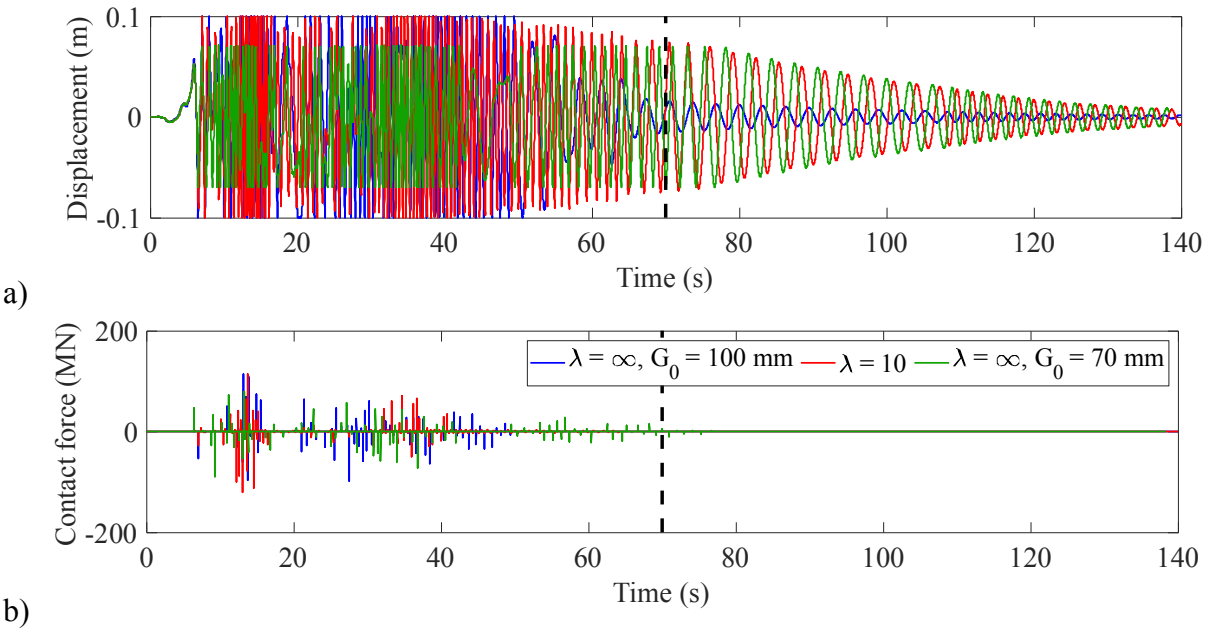

Figure 9: Seismic response for Chi-Chi earthquake for $T_n = 3.00$ s varying the type of impact, a) relative displacement of the roof; b) total contact force.

There are cases where, for some values of λ and k_S, higher contact forces than the hard impact are obtained. These are the cases where the deformation space of the bumper is completely saturated. An example is shown in Fig. 9, where the time histories of the relative displacements of the roof and contact force are shown for the cases of soft impact with $\lambda = 10$ and $T_n = 3.00$ s, hard impact with $G_0 = 100$ mm, and hard impact with $G_0 = 70$ mm for the Chi-Chi earthquake.

Implicitly there is also a comparison between hard impact obtained with different gaps. In all cases, reducing the gap leads to a decrease in the $F_{C,\max}$, while increases the number of impacts n_I. Therefore, in order to reduce the maximum contact forces, it may not be sufficient to vary the gap only, since the values of $F_{C,\max}$ in the two limit cases are comparable. In general, the maximum contact forces are recorded for the case of 100 mm gap and rigid stop.

EARTHQUAKE		Chi-Chi				Northridge			
	T_n [s]	3.00	2.25	1.50	0.75	3.00	2.25	1.50	0.75
λ=10	n_I	161	113	105	60	101	64	116	51
	$F_{C,max}$ [MN]	120.2	69.5	15.1	14.1	98.8	114.2	128.7	38.2
λ=100	n_I	153	160	125	71	48	40	95	54
	$F_{C,max}$ [MN]	12.9	27.1	40.6	42.8	23.4	38.2	42.5	106.0
λ=300	n_I	213	182	147	77	139	90	80	75
	$F_{C,max}$ [MN]	30.5	37.5	46.4	59.1	47.3	43.1	82.4	99.5
λ=600	n_I	201	164	97	73	199	65	71	48
	$F_{C,max}$ [MN]	36.7	52.3	42.4	40.3	64.3	66.6	97.1	66.2
λ=1000	n_I	134	200	163	37	48	29	47	28
	$F_{C,max}$ [MN]	45.2	78.8	72.9	77.7	147.9	79.2	105.9	75.7
λ=∞	n_I	89	82	89	37	62	24	54	25
	$F_{C,max}$ [MN]	88.7	92.7	99.57	72.3	162.8	64.3	106.0	76.1

Table 5: Number of impacts and maximum contact force as a function of the different stiffnesses of the sealing system and λ values for the two earthquakes.

However, it is shown that the use of deformable elements, i.e. acting on the stiffness of the bumpers, not only avoids the impact between two metal parts, but also reduces the maximum contact force by an order of magnitude.

7 CONCLUSIONS

In this paper, a preliminary study of the horizontal dynamics of the floating roof of tanks subjected to seismic action at the base is shown.

The tank parameters that affect the horizontal dynamics of the floating roof are the roof mass, the stiffness and damping of the sealing system, the stiffness and damping of the bumper bars, and the initial gap. A simplified and reduced finite element model was developed, based on the hypothesis of decoupling between horizontal and vertical motion of the roof.

Parametric analyses were performed for two earthquakes by varying the stiffness of the sealing system, the stiffness of the bumpers, and the initial gap, keeping the damping constant.

First, the impact was made elastic hard. With fixed damping and the real initial gap, the seismic responses showed that the more deformable the sealing system, the greater the contact forces and the recentering time of the floating roof. Therefore, acting on the stiffness of the sealing system only, can prevent the impact and limit the magnitude of the contact forces.

Next, the bumper bars were considered partially deformable to obtain an elastic soft impact. The parametric analyses were conducted by varying λ, the ratio between the stiffness of the bumper and that of the sealing system, for the different stiffness values of the sealing system,

keeping the damping of the sealing system fixed and that of the bumper zero. Here, the initial gap was assumed to be smaller than the real gap. In most cases, lambda λ between 10 and 100 provided a reduction of the maximum contact force. There are also cases where the deformation space of the bumper is completely saturated, even for the same λ values.
The maximum contact force is also reduced while the number of impacts is increased by reducing the initial gap in elastic hard impacts.
The variability of these results demonstrates the need for extensive investigations on many more earthquakes. It would also be desirable to further investigate the role of damping, both of the sealing system and of the bumper bars. In particular, damping can be a key aspect in the prevention and mitigation of major accidents, as well as during operation. Optimal design of the parameters characterizing the horizontal dynamics of the roof may result in a reduction of the maximum contact force, the number of impacts, and the recentering time of the floating roof.

ACKNOWLEDGEMENT

INAIL (Italian National Institute for Insurance against Accidents at Work) is funding PhD scholarship for author Michela Salimbeni.

REFERENCES

[1] A.S. Kiremidjian, K. Ortiz, R. Nielsen, and B. Safavi, Seismic risk to major industrial facilities. Report - Stanford University, John A. Blume Earthquake Engineering Center, **72**, 1985.

[2] E. Krausmann, V. Cozzani, E. Salzano, and E. Renni, Industrial accidents triggered by natural hazards: An emerging risk issue. *Natural Hazards and Earth System Science*, **11**, 921–929, 2011.

[3] S. Young, L. Balluz, and J. Malilay, Natural and technologic hazardous material releases during and after natural disasters: A review. *Science of the Total Environment*, **322**, 3–20, 2004.

[4] F. Paolacci, R. Giannini, M. de Angelis, and M. Ciucci. Seismic vulnerability of major-hazard industrial plants and applicability of innovative seismic protection systems for its reduction. *11th World Conference on Seismic Isolation, Energy Dissipation and Active Vibration Control of Structures*, Guangzhou, China, Nov. 17-21, 2009.

[5] P. Moshashaei, S.S. Alizadeh, L. Khazini, and M. Asghari-Jafarabadi, Investigate the Causes of Fires and Explosions at External Floating Roof Tanks: A Comprehensive Literature Review. *Journal of Failure Analysis and Prevention*, **17**, 1044–1052, 2017.

[6] B.L.S. Jacobsen, Impulsive hydrodynamics of fluid inside a cylindrical tank and of fluid surrounding a cylindrical pier. *Bulletin of the Seismological Society of America*, **39**, 189–204, 1949.

[7] K. Senda, On the Vibration of an Elevated Water-Tank I. *Technical Reports of Osaka University*, **117**, 247–264, 1954.

[8] K. Nakagawa, On the vibration of an elevated water tank II. *Technical Reports of Osaka University*, **5**, 1955.

[9] F. Sakai, M. Nishimura, and H. Ogawa, Sloshing behavior of floating-roof oil storage tanks. *Computers & Structures*, **19**, 183–192, 1984.

[10] Y. Yamauchi, A. Kamei, S. Zama, and Y. Uchida, Seismic design of floating roof of oil storage tanks under liquid sloshing. *Proceedings of ASME 2006 Pressure Vessels and Piping Division Conference*, 2006.

[11] M.A. Goudarzi, Seismic behavior of a single deck floating roof due to second sloshing mode. *Journal of Pressure Vessel Technology, Transactions of the ASME*, **135**, 1–6, 2013.

[12] T. Matsui, Sloshing in a cylindrical liquid storage tank with a floating roof under seismic excitation. *Journal of Pressure Vessel Technology, Transactions of the ASME*, **129**, 557–566, 2007.

[13] T. Matsui, Sloshing in a cylindrical liquid storage tank with a single-deck type floating roof under seismic excitation. *Journal of Pressure Vessel Technology, Transactions of the ASME*, **131**, 2009.

[14] R. Shabani and F.G. Golzar, Large deflection analysis of floating roofs subjected to earthquake ground motions. *Nonlinear Analysis: Real World Applications,* **13**, 2034–2048, 2012.

[15] M. Hosseini, A. Soroor, A. Sardar, and F. Jafarieh, A simplified method for seismic analysis of tanks with floating roof by using finite element method: Case study of Kharg (Southern Iran) island tanks. *Procedia Engineering*, **14**, 2884–2890, 2011.

[16] S. Caprinozzi, F. Paolacci, and M. Dolšek, Seismic risk assessment of liquid overtopping in a steel storage tank equipped with a single deck floating roof. *Journal of Loss Prevention in the Process Industries*, **67**, 2020.

[17] H. Ahmadi and M.H. Kadivar, Vibration Analysis of Double Deck Floating Roof of Storage Tank in Cases of Tube, Ordinary and Thickened Foam Seals. *International Journal of Engineering, Transactions A: Basics*, **35**, 1398–1415, 2022.

[18] A. Marino, M. Ciucci, and F. Paolacci, Smart technologies for integrated natural risk management: Innovative methodologies and remote sensing. *Proceedings of ASME 2017 Pressure Vessels and Piping Division Conference*, 2017.

[19] F. Paolacci, R. Giannini, M. De Angelis, and M. Ciucci, Experimental investigation on the seismic behaviour of base-isolated steel storage tank. *11th World Conference on Seismic Isolation, Energy Dissipation and Active Vibration Control of Structures,* Guangzhou, China, Nov. 17-21, 2009.

[20] D. Zahedin Labaf, M. De Angelis, and M. Basili. Multi-objective optimal design and seismic assessment of an inerter-based hybrid control system for storage tanks. *Bulletin of Earthquake Engineering*, **21**, 1481–1507, 2023.

[21] D. Pietrosanti, M. De Angelis, and A. Giaralis. Experimental seismic performance assessment and numerical modelling of nonlinear inerter vibration absorber (IVA)-equipped base isolated structures tested on shaking table. *Earthquake Engineering & Structural Dynamics*, **50**, 2732–2753, 2021.

[22] U. Andreaus, P. Baragatti, M. De Angelis, and S. Perno,. Shaking table tests and numerical investigation of two-sided damping constraint for end-stop impact protection. *Nonlinear Dynamics*, **90**, 2387–2421, 2017.

[23] U. Andreaus, P. Baragatti, M. De Angelis, and S. Perno. A Preliminary Experimental Study about Two-Sided Impacting SDOF Oscillator under Harmonic Excitation. *Journal of Computational and Nonlinear Dynamics*, **12**, 2017.